Supramolecular Gel Phase Controlled [4+2] Diels–Alder Photocycloaddition for Electroplex Mediated White Electroluminescence

4 authors, including:

Satyajit Das
KTH Royal Institute of Technology
10 PUBLICATIONS   **55** CITATIONS

SEE PROFILE

Ayyappanpillai Ajayaghosh
National Institute for Interdisciplinary Science and Technology
267 PUBLICATIONS   **16,961** CITATIONS

SEE PROFILE

Some of the authors of this publication are also working on these related projects:

Design, fabrication and optimization of microfluidic devices for organic synthesis, biological studies, droplet microfluidics and optofluidic applications View project

Light Harvesting Supramolecular Gels View project

Supramolecular Gel Phase Controlled [4 + 2] Diels−Alder Photocycloaddition for Electroplex Mediated White Electroluminescence

Satyajit Das,[†,‡] Naoki Okamura,[§] Shigeyuki Yagi,[§] and Ayyappanpillai Ajayaghosh*[,†,‡]

[†]Photosciences and Photonics Section, Chemical Sciences and Technology Division, CSIR-National Institute for Interdisciplinary Science and Technology (CSIR-NIIST), Thiruvananthapuram 695019, India
[‡]Academy of Scientific and Innovative Research (AcSIR), Ghaziabad 201002, India
[§]Department of Applied Chemistry, Graduate School of Engineering, Osaka Prefecture University, 1-1 Gakuen-cho, Naka-ku, Sakai, Osaka 5999-8531, Japan

Ⓢ *Supporting Information*

ABSTRACT: Diels−Alder photocycloaddition of 9-phenylethynylanthracene results in multiple [4 + 2] and [4 + 4] cycloaddition products in solution, which can be controlled to form specific products under a restricted environment. We have exploited the gel phase of a 9-phenylethynylanthracence derivative as a confined medium to specifically yield the [4 + 2] cycloadduct in >90% yield. The photocycloadduct (*anti*-form) exhibited a blue emission with CIE chromaticity of $x = 0.16/y = 0.16$. Construction of an organic light emitting device with the photocycloadduct, using a carbazole-based hole transporting host, resulted in white light emission with a CIE chromaticity of $x = 0.33/y = 0.32$. This observation not only highlights the use of gel chemistry to achieve the otherwise difficult to obtain photoproducts but also underlines their potential in optoelectronic device fabrication.

Confinement of molecular systems yielding regio- and stereospecific reaction products has been reported in several cases.[1] An example is the Diels−Alder photocycloaddition of anthracene[2] and its 9-phenylethynyl derivative.[3] While anthracene results in *anti* and *syn* isomers of [4 + 4] photocycloadducts in the absence of oxygen,[4,5] 9-phenylethynylanthracene in principle should form four different products (Scheme 1). Though these products are allowed by selection rules, the unfavorable geometries enable only [4 + 2]-*anti* (64%) and [4 + 4] *anti* (23%) addition.[3,6] However, energetically unfavorable products were specifically obtained under confined conditions.[7,8] The majority of these reports have been limited to the synthesis of selective products on confined surfaces; however, practical application of these types of products are yet to be demonstrated.[9]

Supramolecular gels have been shown to be a suitable medium for crystallization of molecules.[10] H-Bonding and π-stacking in the gel state have an advantage over the solution state to obtain certain stereospecific products in high yield.[11] Herein, we establish that molecular self-assembly and gel chemistry can be used to control Diels−Alder photocycloaddition to achieve a specific product in high yield,

Scheme 1. Photocycloaddition of 9-Phenylethynylanthracene in Solution[6,7]
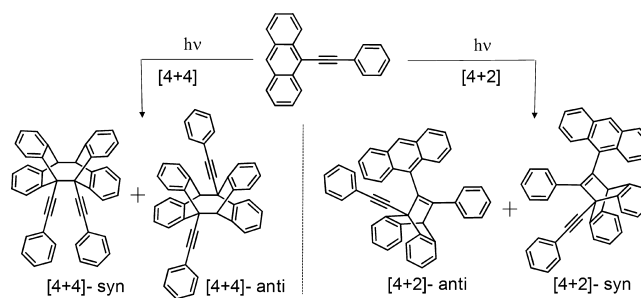
which can be used for fabricating white light emitting devices. Though white light emission is a topic of current interest in lighting applications,[12−14] single molecular white electroluminescence is rarely observed.[14,15] Electromer and electroplex formation by the emitting species and the hole transporting material is the reason for white electroluminescence.[14a,15] Such electrically excited complexes are akin to excimers and exciplexes observed in the case of photoluminescence and have long wavelength mixed emission, providing balanced color coordinates required for white light emission.
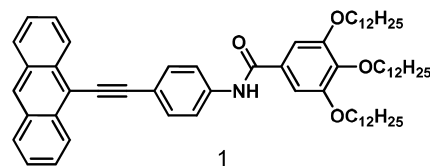
In this study, a 9-phenylethylanthracene derivative **1** was designed which facilitates H-bonded self-assembly[16] in methyl cyclohexane (MCH, 3.3 μM, Figure S1a). Plots of the fraction of aggregate (α_{agg}) against the temperature could be fitted to a cooperative self-assembly pathway. The enthalpy of nucleation of the assembly (ΔH_{nucl}) was found to be −9 kJ/mol, and the elongation temperature was 303 K (Figure S1b and Table S1).

The molecule **1** in hot MCH (1.19 w/v) upon sonication and cooling resulted in a reversible gel (Figure 1a,b) having a
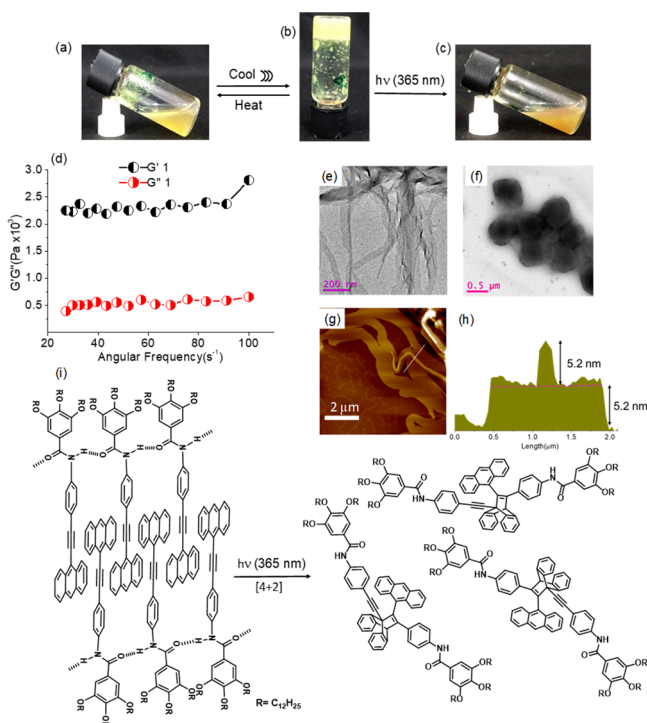

Figure 1. (a, b) Photographs showing reversible gelation of **1** in MCH and (c) the gel after photoirradiation. (d) Rheological behavior of the gel. (e, f) TEM images of the gel before and after photoirradiation. (g) AFM image of the self-assembled **1** in MCH. (h) The height profile. (i) Molecular assembly and structural change of **1** before and after photoirradiation.

storage modulus (G') of **1** order of magnitude greater than that of the loss modulus (G'') (Figure 1d). Atomic force microscopy (AFM) and transmission electron microscopy (TEM) analyses revealed a tapelike morphology (Figures 1e, S2, and S3). X-ray diffraction (XRD) of the xerogel exhibited peaks corresponding to *d*-spacing of 47.9, 21.5, and 12.5 Å. First three peaks followed the reciprocal relationship with a ratio of 1:∼2:∼4, which correspond to multidimensional lamellar packing. The peaks corresponding to 3.82 and 4.20 Å indicate π-stacking and long-range ordered intermolecular H-bonding, respectively. The peaks corresponding to 8.69, 8.28, 7.49, 6.91, 6.31, 5.80, and 5.28 Å represent the interdigitated H-bonded assembly where the anthracene moiety of the molecule is overlapped with the triple bond (Figures 1 and S4). This is evident from temperature controlled absorption changes in the 230–260 nm region (Figure S5a), where the band corresponding to the ^1B_b transition dipole of anthracene, parallel to the molecular axis, is not being polarized via aggregation and remained nearly unsplit.[17] The steady state fluorescence spectrum (Figure S5b) of the gel did not show excimer emission,[18] as supported by a time correlated single photon counting experiment (Figure S5c). The fluorescence decay profile of the gel was fitted with a biexponential decay having lifetime values of 1.95 and 4.00 ns.

The absence of any emissive species with a lifetime value of >10 ns indicates that no prominent overlap between two anthracene cores are present in the molecular assembly. The thickness of a single layered sheet evaluated by AFM analysis is

5.2 nm, corresponding to a monolayer of the assembly (Figure 1g, h). The interdigitated long-range arrangement of **1** is ideally suited for the specific [4 + 2] Diels−Alder photo-reaction (Figure 1i) as established by the irradiation of a gel of the molecule **1**, with 365 nm light. In the process, the gel turned into a solution (Figure 1c), which could not be reversed to a gel by irradiation at shorter wavelength or by cooling.

The HPLC profile of the irradiated solution showed a major peak corresponding to a 91% conversion of the starting compound (Figure S6a). The ^1H NMR profile of the photoirradiated gel suggested 90−92% formation of photo-adduct (Figure S6b), whereas the xerogel and the solution state photoreaction showed low conversion and less stereo-selectivity, respectively (Figure S7). The ^1H NMR and NOESY spectra confirmed the *anti*-[4 + 2] cycloaddition (Figures S8, S9). This geometry disturbs the assembly of the molecule resulting in the dissolution of the gel. AFM and TEM analyses of the photoadduct showed ill-defined particles as shown in Figures 1f and S10b, justifying the destruction of the one-dimensional H-bonded assembly of the gel phase. This observation is confirmed by the XRD analysis of the gel after photoirradiation, which shows a decrease in the number of diffraction peaks (Figure S10). Comparison of the FT-IR spectra (Figure S11) before and after photoirradiation revealed that the H-bonded N−H stretching frequency of the gel (ν_{N-H} = 3261 cm^{-1}) was shifted to 3279 cm^{-1} which is close to the monomeric state (3284 cm^{-1}), indicating the breakage of the H-bonding.

The absorption and emission features of the gelator **1** and its photoadduct in chloroform (3.3 μM) are shown in Figure 2a−
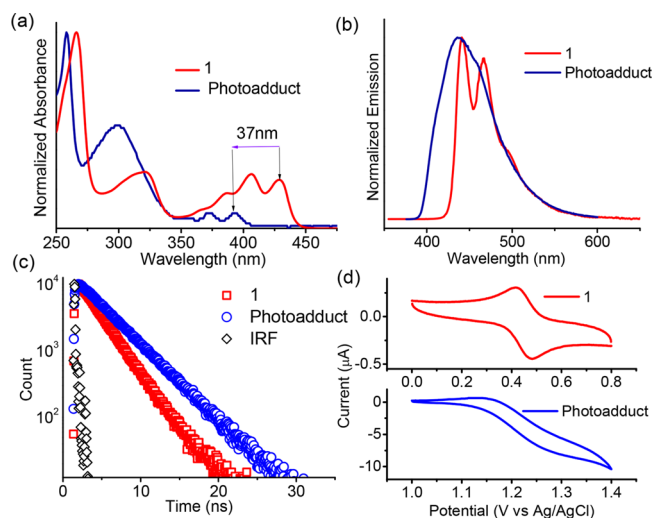

Figure 2. Comparative properties of **1** (red) and photoproduct (blue). (a) Absorption, (b) emission, and (c) fluorescence lifetime decay profiles in chloroform and (d) cyclic voltammograms in dichloromethane.

c. The absorption spectrum of **1** showed peaks at 266, 323, 366, 386, 406, and 429 nm. However, in the case of the photoadduct, the absorption bands at 429 and 406 nm disappeared with the appearance of two relatively less intense bands at 393 and 373 nm and an intense band at 299 nm. The gelator **1** exhibited two intense emission peaks at 450 and 475 nm, whereas the photoadduct showed an emission with a maximum at 440 nm. The fluorescence quantum yields of **1** and the photoadduct were 0.79 and 0.57, respectively. The

fluorescence lifetime analysis of **1** and its photoadduct in chloroform exhibited a single exponential decay with lifetime values of 2.91 and 4.28 ns, respectively (Figure 2c).

Cyclic voltammograms of **1** and the photoadduct (Figure 2d) suggest that the E_{HOMO} of the photoadduct is (−5.54 eV) more stabilized than that of the gelator **1** (−4.79 eV) due to loss of extended π-conjugation (Figures S12, S13). A similar observation has been made in the E_{LUMO} of the photoadduct (−2.59 eV) and **1** (−1.98 eV) as tabulated in Table S2. The device characteristics of the gelator **1** were investigated by fabricating solution processed single layer organic light emitting devices (Figure S14).[19a] The emitting layer (EML) comprised the gelator **1**, the carbazole derivative PVCz or SB2[19b] as the hole transporting material (HTM), and the oxadiazole derivative PBD as the electron transporting material (ETM). PVCz was a better HTM than SB2 as indicated by the higher L_{max} value of the devices with the former (Table S3). The intensity of the EL spectra increased upon increasing the applied voltage; however, the structure of the spectra remained unchanged. The L_{max} obtained for the **1**+PVCz was 1244 cd/m² at 16.5 V and 231 cd/m² for **1**+SB2 at 14.5 V. In both cases, blue EL with CIE coordinates of (0.16, 0.16) and (0.16, 0.13), respectively, were obtained and remained almost constant at any applied voltages (Figure 3a,c,e,f).

Interestingly, the device fabricated using the photoirradiated gelator with PVCz (or SB2) as the EML and PBD as the ETM exhibited broad EL spectra between 400 and 750 nm, with maxima at 445 and 573 nm (Figure 3b,d), resulting in white electroluminescence. The performance of the PVCz based
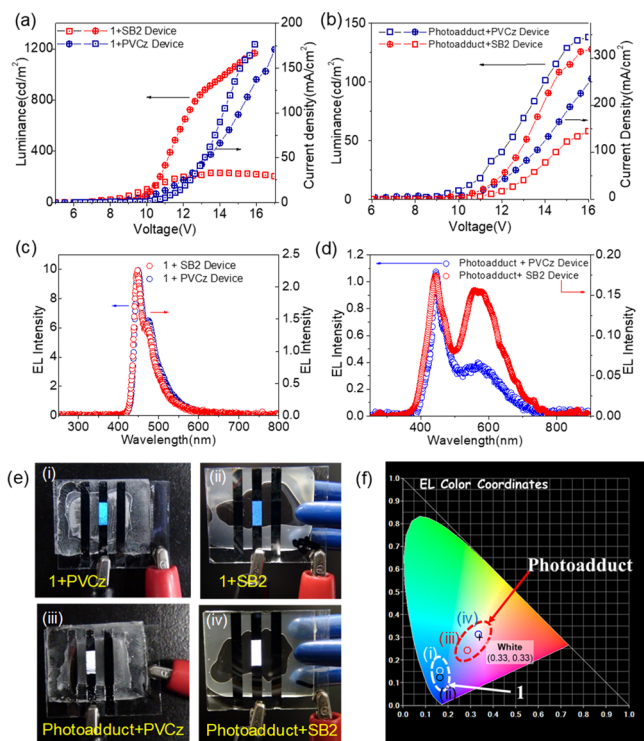
device is better when compared to that with SB2. The structure of the EL spectra remained unchanged while the intensity increased with the increase in the voltage (Figures S15, S16). When SB2 was used as the HTM, the CIE coordinate of the white light emission was $x = 0.33/y = 0.32$, indicating high color purity. On the other hand, the value of the CIE coordinates was $x = 0.28/y = 0.25$ when PVCz was used as the HTM (Figure 3e,f).

For a deeper understanding of the origin of the white electroluminescence, the EL and PL spectra of the devices fabricated with the gelator **1** before and after photoirradiation using PVCz and SB2 as the HTM were compared (Figure 4a–
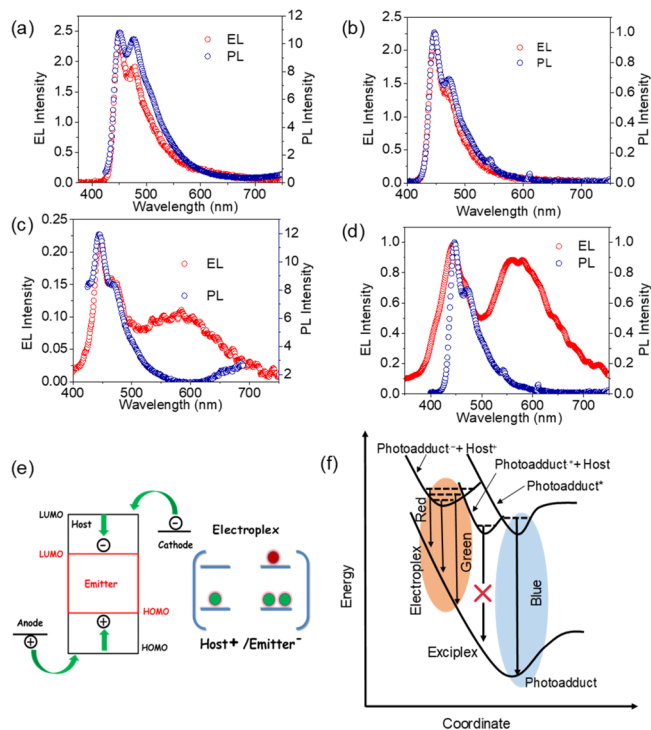
Figure 4. Comparative PL and EL spectra of devices made of (a) 1+PVCz, (b) 1+SB2, (c) photoadduct+PVCz, and (d) photoadduct+SB2. (e) Schematic representation of the electronic configuration in molecular orbitals of the electroplex host/emitter. (f) Proposed energy profile for the electroluminescence response of the photoadduct, exciplex, and electroplex.

Figure 3. Device characteristics (luminance and current density vs voltage plot) of (a) **1** and (b) photoadduct. Electroluminescence spectra of OLED made of (c) **1** and (d) photoadduct as emitter with SB2 (red) and PVCz (blue) as hole-transporting materials. (e) Photographs of electroluminescent devices fabricated with the gelator **1** (i, ii) and photoadduct (iii, iv). (f) EL color coordinates with the devices made of **1** and the photoadduct.

d). Both EL and PL spectra of the gelator before photoirradiation are comparable, which exhibited blue emission with maxima at 450 and 470 nm. Similarly, the PL spectra of the devices fabricated using both PVCz and SB2 as the HTM showed blue emission with a maximum at 450 nm and a shoulder band at 475 nm. However, the EL spectra in both cases exhibited a broad emission at 600 nm, in addition to the sharp emission at 450 nm. Notably the intensity of the broad 600 nm emission was less when PVCz was used as the HTM.

Since the PL emission of the photoirradiated gelator was blue, we expected a similar emission characteristic for the EL spectrum as well. Instead, we observed an electrogenerated white light emission, which may not be the property of the photoadduct alone. Furthermore, the film state absorption of EML did not show any new band in the presence of the photoadduct (Figure S17), which is an indication of the absence of ground state charge transfer between the emitter and the HTM. Therefore, the green and red emission required

for the white emission must have generated through the interaction between the photoadduct and the transporting materials under the applied electric field. Probably, an electron transfer from the HTM to the photoadduct could generate an excited complex called electroplex, similar to a photoexcited exciplex (Figure 4e). Such an emission by the electrically excited electroplex can be visible only by an EL spectrum and not by a photoexcited PL spectrum.[15a]

The energy level of the electroplex is lower than that of the singlet excited state of the photoadduct (Figure 4e). This electroplex (photoadduct⁻ + HTM⁺) formation is in analogy with previous reports and should be responsible for the green-to-red emission along with the blue emission of the photoadduct, leading to the white light emission (Figure 4f).[15,20] To establish the electroplex formation between the emitter and the HTM, we fabricated devices by mixing them together with an electron transporting layer ([1,1′:3′,1″-terphenyl]-4,4″-diylbis(diphenylphosphine oxide), BPOBP)[21] separately coated in solution processed double layer devices (Figure S18). As expected, the device with emitter **1** showed blue emission, whereas the device made out of the photo-irradiated gelator exhibited white light emission, underlining the electroplex formation between the photoadduct and the carbazole-based compounds (Figure S19). The role of the [4 + 2] photocycloadduct in the electroplex formation is confirmed by the comparatively weak bluish-white electroluminescence with a photoirradiated 9-phenylethynyleneanthracene (9PEA) having a mixture of photoadducts (Figure S20).

In conclusion, the gel phase of the molecule **1** creates enough confinement, selectively yielding the [4 + 2] photocycloadduct. Light emitting devices fabricated with the gelator **1** exhibited a blue emission, whereas the device fabricated with the photoirradiated gelator showed a white electroluminescence. The generation of the green and red emission required for white luminescence is explained on the basis of an electroplex formation between the photo-cycloadduct and the hole transporting material within the device structure under an applied electric potential. This report highlights the role of H-bonded supramolecular assembly and gelation of functional molecules to achieve exclusive photo-products for their use in photonic device application.

ASSOCIATED CONTENT

Ⓢ Supporting Information

The Supporting Information is available free of charge on the ACS Publications website at DOI: 10.1021/jacs.9b00955.

General methods, synthetic procedures, gelation, photo-irradiation, OLED fabrication, and additional figures (PDF)

AUTHOR INFORMATION

Corresponding Author

*ajayaghosh@niist.res.in

ORCID Ⓞ

Ayyappanpillai Ajayaghosh: 0000-0001-8574-5391

Notes

The authors declare no competing financial interest.

ACKNOWLEDGMENTS

REFERENCES

(1) (a) Yoshizawa, M.; Klosterman, J. K.; Fujita, M. Functional Molecular Flasks: New Properties and Reactions within Discrete, Self-Assembled Hosts. *Angew. Chem., Int. Ed.* **2009**, *48*, 3418−3438. (b) Ramamurthy, V.; Sivaguru, J. Supramolecular Photochemistry as a Potential Synthetic Tool: Photocycloaddition. *Chem. Rev.* **2016**, *116*, 9914−9993.

(2) (a) Becker, H.-D. Unimolecular Photochemistry of Anthracenes. *Chem. Rev.* **1993**, *93*, 145−172. (b) Bouas-Laurent, H.; Castellan, A.; Desvergne, J.-P.; Lapouyade, R. Photodimerization of Anthracenes in Fluid Solution: Structural Aspects. *Chem. Soc. Rev.* **2000**, *29*, 43−55.

(3) Becker, H. D.; Andersson, K. Photochemical Diels—Alder Dimerization of 9-Phenylethylnylanthracene. *J. Photochem.* **1984**, *26*, 75−77.

(4) (a) Aubry, J.-M.; Pierlot, C.; Rigaudy, J.; Schmidt, R. Reversible Binding of Oxygen to Aromatic Compounds. *Acc. Chem. Res.* **2003**, *36*, 668−675. (c) Fudickar, W.; Linker, T. Why Triple Bonds Protect Acenes from Oxidation and Decomposition. *J. Am. Chem. Soc.* **2012**, *134*, 15071−15082.

(5) (a) Nakamura, A.; Inoue, Y. Supramolecular Catalysis of the Enantiodifferentiating [4 + 4] Photocyclodimerization of 2-Anthracenecarboxylate by γ-Cyclodextrin. *J. Am. Chem. Soc.* **2003**, *125*, 966−972. (b) Fukuhara, G.; Iida, K.; Kawanami, Y.; Tanaka, H.; Mori, T.; Inoue, Y. Excited-State Dynamics Achieved Ultimate Stereocontrol of Photocyclodimerization of Anthracenecarboxylates on a Glucose Scaffold. *J. Am. Chem. Soc.* **2015**, *137*, 15007−15014.

(6) Tanabe, J.; Taura, D.; Ousaka, N.; Yashima, E. Remarkable Acceleration of Template-directed Photodimerisation of 9-phenyl-ethynylanthracene Derivatives Assisted by Complementary Salt Bridge Formation. *Org. Biomol. Chem.* **2016**, *14*, 10822−10832.

(7) (a) Kim, M.; Hohman, J. N.; Cao, Y.; Houk, K. N.; Ma, H.; Jen, K.-Y. A.; Weiss, P. S. Creating Favorable Geometries for Directing Organic Photoreactions in Alkanethiolate Monolayers. *Science* **2011**, *331*, 1312−1315. (b) Zheng, Y. B.; Payton, J. L.; Song, T.-B.; Pathem, B. K.; Zhao, Y.; Ma, H.; Yang, Y.; Jensen, L.; Jen, A. K.-Y.; Weiss, P. S. Surface-enhanced Raman Spectroscopy to Probe Photoreaction Pathways and Kinetics of Isolated Reactants on Surfaces: Flat Versus Curved Substrates. *Nano Lett.* **2012**, *12*, 5362−5368.

(8) Zdobinsky, T.; Maiti, P. S.; Klajn, R. Support Curvature and Conformational Freedom Control Chemical Reactivity of Immobilized Species. *J. Am. Chem. Soc.* **2014**, *136*, 2711−2714.

(9) Weber, M. D.; Adam, M.; Tykwinski, R. R.; Costa, R. D. Controlling the Chromaticity of Small-Molecule Light-Emitting Electrochemical Cells Based on TIPS-Pentacene. *Adv. Funct. Mater.* **2015**, *25*, 5066−5074.

(10) (a) Babu, S. S.; Praveen, V. K.; Ajayaghosh, A. Functional π-gelators and Their Applications. *Chem. Rev.* **2014**, *114*, 1973−2129. (b) Jones, C. D.; Steed, J. W. Gels with Sense: Supramolecular Materials that Respond to Heat, Light and Sound. *Chem. Soc. Rev.* **2016**, *45*, 6546−6596. (c) Nair, V. S.; Mukhopadhyay, R. D.; Saeki, A.; Seki, S.; Ajayaghosh, A. A π-gel scaffold for assembling fullerene to photoconducting supramolecular rods. *Sci. Adv.* **2016**, *2*, No. e1600142.

(11) (a) Dawn, A.; Fujita, N.; Haraguchi, S.; Sada, K.; Shinkai, S. An Organogel System can Control the Stereochemical Course of Anthracene Photodimerization. *Chem. Commun.* **2009**, *0*, 2100−2102. (b) Dawn, A.; Shiraki, T.; Ichikawa, H.; Takada, A.; Takahashi, Y.; Tsuchiya, Y.; Lien, L. T. N.; Shinkai, S. Stereochemistry-dependent, Mechanoresponsive Supramolecular Host Assemblies for Fullerenes: a Guest-induced Enhancement of Thixotropy. *J. Am. Chem. Soc.* **2012**, *134*, 2161−2171.

(12) Ying, L.; Ho, C.-L.; Wu, H.; Cao, Y.; Wong, W.-Y. White Polymer Light-emitting Devices for Solid-state Lighting: Materials, Devices, and Recent Progress. *Adv. Mater.* **2014**, *26*, 2459−2473.

(13) (a) Chen, Y.-H.; Tang, K.-C.; Chen, Y.-T.; Shen, J.-Y.; Wu, Y.-S.; Liu, S.-H.; Lee, C.-S.; Chen, C.-H.; Lai, T.-Y.; Tung, S.-H.; Jeng, R.-J.; Hung, W.-Y.; Jiao, M.; Wu, C.-C.; Chou, P.-T. Insight into the Mechanism and Outcoupling Enhancement of Excimer-associated White Light Generation. *Chem. Sci.* **2016**, *7*, 3556−3563. (b) Xu, B.; Wu, H.; Chen, J.; Yang, Z.; Yang, Z.; Wu, Y.-C.; Zhang, Y.; Jin, C.; Lu, P.-Y.; Liu, S.; Xu, J.; Aldred, M. White-light Emission from a Single Heavy Atom-free Molecule with Room Temperature Phosphorescence, Mechanochromism and Thermochromism. *Chem. Sci.* **2017**, *8*, 1909−1914.

(14) (a) Liu, Y.; Nishiura, M.; Wang, Y.; Hou, Z. π-Conjugated Aromatic Enynes as a Single-Emitting Component for White Electroluminescence. *J. Am. Chem. Soc.* **2006**, *128*, 5592−5593. (b) Okamura, N.; Maeda, T.; Fujiwara, H.; Soman, A.; Unni, K. N. N.; Ajayaghosh, A.; Yagi, S. Photokinetic Study on Remarkable Excimer Phosphorescence from Heteroleptic Cyclometalated Platinum(II) Complexes Bearing a Benzoylated 2-phenylpyridinate Ligand. *Phys. Chem. Chem. Phys.* **2018**, *20*, 542−552. (c) Okamura, N.; Egawa, K.; Maeda, T.; Yagi, S. Control of Excimer Phosphorescence by Steric Effects in Cyclometalated Platinum(II) Diketonate Complexes Bearing Peripheral Carbazole Moieties towards Application in Non-doped White OLEDs. *New J. Chem.* **2018**, *42*, 11583−11592.

(15) (a) Berggren, M.; Gustafsson, G.; Inganäs, O.; Andersson, M. R.; Hjertberg, T.; Wennerström, O. White light from an electroluminescent diode made from poly[3(4-octylphenyl)-2,2'-bithiophene] and an oxadiazole derivative. *J. Appl. Phys.* **1994**, *76*, 7530−7534. (b) Li, J. Y.; Liu, D.; Ma, C.; Lengyel, O.; Lee, C.-S.; Tung, C.-H.; Lee, S. White-Light Emission from a Single-Emitting-Component Organic Electroluminescent Device. *Adv. Mater.* **2004**, *16*, 1538−1541. (c) Zhao, Z.; Xu, B.; Yang, Z.; Wang, H.; Wang, X.; Lu, P.; Tian, W. White Light from Excimer and Electromer in Single-Emitting-Component Electroluminescent Diodes. *J. Phys. Chem. C* **2008**, *112*, 8511−8515. (d) Wen, L.; Li, F.; Xie, J.; Wu, C.; Zheng, Y.; Chen, D.; Xu, S.; Guo, T.; Qu, B.; Chen, Z.; Gong, Q. Electroplex emission at PVK/Bphen interface for application in white organic light-emitting diodes. *J. Lumin.* **2011**, *131*, 2252−2254. (e) Luo, D.; Li, X.-L.; Zhao, Y.; Gao, Y.; Liu, B. High-Performance Blue Molecular Emitter-Free and Doping-Free Hybrid White Organic Light-Emitting Diodes: an Alternative Concept To Manipulate Charges and Excitons Based on Exciplex and Electroplex Emission. *ACS Photonics* **2017**, *4*, 1566−1575.

(16) Lubtow, M.; Helmers, I.; Stepanenko, V.; Albuquerque, R. Q.; Marder, T. B.; Fernandez, G. Self-Assembly of 9,10-Bis-(phenylethynyl) Anthracene (BPEA) Derivatives: Influence of π−π and Hydrogen-Bonding Interactions on Aggregate Morphology and Self-Assembly Mechanism. *Chem. - Eur. J.* **2017**, *23*, 6198−6205.

(17) Ando, Y.; Sugihara, T.; Kimura, K.; Tsuda, A. A Self-Assembled Helical Anthracene Nanofibre Whose P- and M-Isomers Show Unequal Linear Dichroism in a Vortex. *Chem. Commun.* **2011**, *47*, 11748−11750.

(18) Sugino, M.; Araki, Y.; Hatanaka, K.; Hisaki, I.; Miyata, M.; Tohnai, N. Elucidation of Anthracene Arrangement for Excimer Emission at Ambient Conditions. *Cryst. Growth Des.* **2013**, *13*, 4986−4992.

(19) (a) Shigehiro, T.; Yagi, S.; Maeda, T.; Nakazumi, H.; Fujiwara, H.; Sakurai, Y. Photo- and Electroluminescence from 2-(Dibenzo-[*b,d*]furan-4-yl)pyridine-Based Heteroleptic Cyclometalated Platinum(II) Complexes: Excimer Formation Drastically Facilitated by an Aromatic Diketonate Ancillary Ligand. *J. Phys. Chem. C* **2013**, *117*, 532−542. (b) Okamura, N.; Funagoshi, H.; Ikawa, S.; Yagi, S.; Maeda, T. Starburst-Type Carbazole Trimers as Host Materials for Solution-Processed Phosphorescent OLEDs. *Mol. Cryst. Liq. Cryst.* **2015**, *621*, 59−63.

(20) (a) Wei, M.; Gui, G.; Chung, Y.-H.; Xiao, L.; Qu, B.; Chen, Z. Micromechanism of Electroplex formation. *Phys. Status Solidi B* **2015**, *252*, 1711−1716. (b) Shin, D.-M. The Characteristics of Electroplex Generated from the Organic Light Emitting Diodes. *J. Nanosci. Nanotechnol.* **2010**, *10*, 6794−6799. (c) Liu, J.; Chou, S.-Y.; Tong, K.; Luan, X.; Zhao, F.; Pei, Q.; Li, H. Study of White Electroluminescence from a Single-Component Polymer Using an Electrolyte-Gated Diode. *J. Phys. Chem. C* **2017**, *121*, 10112−10118. (d) Li, J.; Xu, Z.; Zhang, F.; Zhao, S.; Song, D.; Zhu, H.; Song, J.; Wang, Y.; Xu, X. Electroplex emission of the blend film of PVK and DPVBi. *Solid-State Electron.* **2010**, *54*, 349−352.

(21) Aizawa, N.; Pu, Y. J.; Watanabe, M.; Chiba, T.; Ideta, K.; Toyota, N.; Igarashi, M.; Suzuri, Y.; Sasabe, H.; Kido, J. Solution-processed multilayer small-molecule light-emitting devices with high-efficiency white-light emission. *Nat. Commun.* **2014**, *5*, 5756.